

Morphological and structural effects of NaOH added to silica

A. BOSSI, G. LEOFANTI, E. MORETTI, N. GIORDANO

Montedison S.p.A., Research Centre of Bollate, Milano, Italy

The effects of addition of NaOH (from 0.5 to 3%) upon the morphological and structural properties of a commercial silica support have been investigated in the range from 300 to 780°C: samples have been characterized by means of surface area, pore volume, pore and particle size distribution measurements, chemical and X-ray analysis, electron and optical microscopy observations. Results of various techniques were allied in showing the prevalency, at the lowest temperatures (< 600°C), of surface modifications involving chemical reaction and incipient sintering while at the highest temperatures (> 600°C) modifications entail the entire mass which undergoes a crystallization process. The singular presence of keatite, not hitherto reported for similar systems, allowed an interpretation of the crystallization process in terms of the sequence:

amorphous → cristobalite → (keatite) → quartz.

1. Introduction

The structural and physical properties of silica gels are known to be greatly affected by addition of a "mineralizer": interest on this subject has produced a large number of published works [1-29] directed toward elucidation of the influence of the nature and concentration of a "mineralizer" as well as of the temperature, pressure and atmosphere of heat-treatment. All related investigations locate regions of variables where either sintering or crystallization occur: as far as we know, there is a lack of comprehensive works which correlate structural with the morphological modifications occurring at lower temperatures. Moreover, while there is general agreement as to the initial act of interaction between the "mineralizer" and the OH groups of silica [5, 7, 10], interpretations related to the subsequent heat-treatment suffer the lack of detailed information on the nature of formed phases and their influence on the sintering and the crystallization processes. Results presented in this paper provide additional information on these subjects, obtained while investigating the interaction of NaOH with a high-surface area silica of the type largely used, as a support, in catalytic systems. Supports of this type have recently found increasing importance in industrial processes, namely in oxidation and

ammoxidation of hydrocarbons: the present work was aimed to show, for one specific case, how added cations can modify the characteristic of the original support, hence how they influence the life of the catalyst on the whole.

Results from various techniques (surface areas, porosimetry, scanning electron and optical microscopy observations, X-ray results, chemical solubility, particle size distribution) were allied in showing a most coherent picture of various modifications occurring within a broad range of temperatures and other variables. Extensive results allowed the possible mechanism underlying the "mineralizer" effect both in the sintering and the crystallization regions to be outlined; the proposed model may also serve as a basis for studies in related and more complex mineralizer-silica systems.

2. Experimental part

2.1. Sample preparation

Preparation of samples containing NaOH was accomplished by impregnation, with known volumes of aqueous solutions of NaOH, of a commercial microspheroidal silica. Samples were dried in an oven at 110°C for 16 h, then were sintered in air at prefixed temperatures for several hours.

Rates of heating and cooling were respectively

100 and 125°C h⁻¹; final values of temperatures were controlled within $\pm 5^\circ\text{C}$. Reference to the various samples will be made by giving with the symbol S (Silica), the weight percentage of NaOH followed by the temperature and time of heat-treatment: thus S-1-600(16) designates a sample of silica containing 1% of NaOH, heat-treated at 600°C for 16 h.

2.2. Physical-chemical characterization

Batches of various samples were withdrawn from the oven at different times and analysed by various techniques, as indicated below. Surface areas were calculated from the amount of nitrogen adsorbed from a nitrogen-helium stream, at liquid nitrogen temperature [30]. Pore volume and pore-size distribution in the range from 37.5 to 75000 Å were measured by a mercury-porosimeter (C. Erba model 70 H). Total pore volume was determined by the water titration method [31]. Particle size distribution was determined by sieving with Micromesh sieves. For chemical analysis weighed amounts of various samples (0.5 g) were digested in water for 4 days and the solutions analysed by atomic adsorption, for content of Na (Na_{sol}) and, by colorimetric method, for soluble Si (Si_{sol}). X-ray powder diffraction patterns were obtained in a Philips apparatus (P.W.1010-1050-1051 type) using $\text{CuK}\alpha$ radiation and Ni filter. Optical and scanning electron microscopy measurements were performed respectively on polarizing Ortholux Leitz microscope and a scanning electron microscope (Stereoscan model Mark 2A).

3. Results

3.1. Surface areas and pore volumes

Results of surface area and pore volume measurements, summarized in Figs. 1a and b, illustrate very clearly the net effect of NaOH addition: morphological properties of Na-loaded silica are in fact more drastically affected by variations in the temperature of pre-treatment than those of pure silica. Modifications induced by NaOH are still evident at the lowest temperature of investigation (300°C), in contrast with pure silica which is stable up to temperatures as high as 900°C. It is noteworthy that, while in the case of pure silica surface areas and pore volumes vary with temperature in a similar way, presence of NaOH has a more pronounced effect upon surface areas (Fig. 1a) than on pore volumes (Fig. 1b).

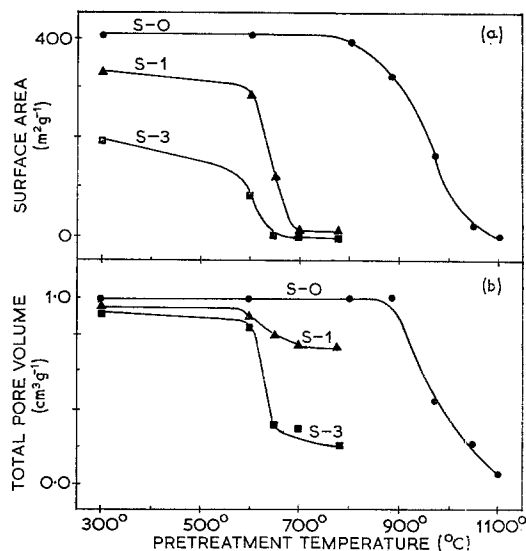


Figure 1 Variation with the pre-treatment temperature of: (a) surface area; (b) total pore volume.

This behaviour is consistent with pore-size distribution curves (Figs. 2a, b and c) which show that NaOH addition causes a progressive increase of pore sizes at increasing pre-treatment temperature: closer appraisal of the curves in

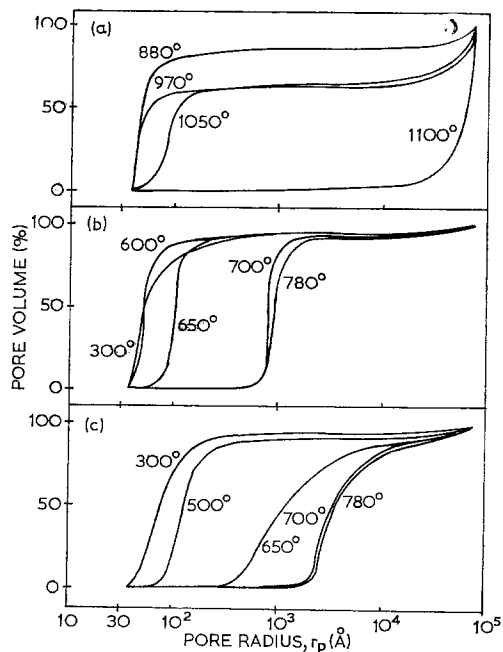


Figure 2 Pore size distribution of the samples activated for 16 h: (a) pure silica; (b) S-1; (c) S-3.

Figs. 2a, b and c indicates that the observed variations are not brought about by filling of the smallest pores but, instead, by true enlargement of the existing ones. From the view-point of influence of NaOH concentration, comparison of the data of Figs. 1 and 2 makes it evident that higher NaOH content causes the more drastic effect upon the morphological properties.

3.2. Particle size distribution

Measurements of particle size distribution have disclosed a new effect of added NaOH, not hitherto reported in the quoted literature: the general behaviour is illustrated in Fig. 3 where the particle size distribution of S-0-300(16), S-0-1100(16) and S-3-700(16) is shown. In the case of pure silica, an increase in the temperature of pre-treatment brings about disaggregation of the original particles, while loading of NaOH on silica causes agglomeration of the particles, as shown by the fractional decrease of the smallest ones.

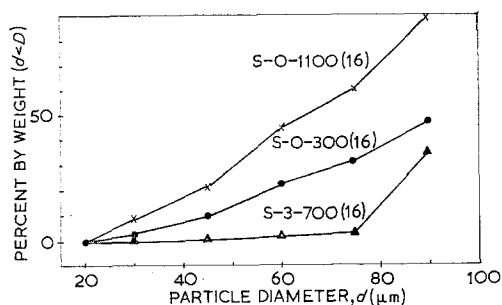


Figure 3 Particle size distribution.

3.3. Solubility measurements

Experimental values of Si_{sol} , corrected for the blank, are reported in Table I together with values of Na_{sol} . A comparison of the results, obtained on the S-3 samples activated at various temperatures (Table I), gives strong evidence in favour of the existence of a discontinuity in the vicinity of 600°C : at this temperature, both the

per cent of Na_{sol} and the $\text{Na}_{\text{sol}}:\text{Si}_{\text{sol}}$ ratio increase indicating a change in the nature of Na-Si interaction. This behaviour could be interpreted by the possible formation, at the lower temperatures, of stable surface silicates hardly soluble in water, while, at the higher temperature, decomposition of silicates prevails with subsequent formation of NaOH as the final product. This hypothesis is consistent with some literature reported for other added cations [8, 13].

3.4. Scanning electron microscope observations

Scanning electron microscope observations help to give confidence to the results of other techniques: thus, while the porous structure of pure silica appears still unchanged even after treatment at 1100°C (Figs. 4a and b), striking differences are evident in the case of the S-3 samples, at much lower temperatures, such as is shown from comparison of the S-3-600(16) and S-3-700(16) samples (Figs. 4c and d). Thus while the S-3-600(16) still retains unchanged its external configuration, large sintering effects, in the case of S-3-700(16), are indicated by formation of large round agglomerates and large cavities within the particle. These differences are consistent with the variations already shown in the surface areas which, too, indicate large sintering effects within this temperature range. Besides, inspection of electron micrographs on some particles reveals the existence of numerous whiskers (Figs. 5a and b) which could be removed simply by leaching with water (Fig. 5c). Heat-treatment up to 780°C did not further alter the sample structure (Fig. 5d) with respect to previous samples in the series (S-3-700(16)), which, therefore, appears to mark the conditions of complete sintering.

3.5. X-ray measurements

X-ray powder patterns of pure silica underline the absence of any crystalline phases and significant transformations up to 1100°C ; by

TABLE I Solubility measurements.

Samples	Na_{sol} ($\gamma \text{ cm}^{-3}$)	Si_{sol} ($\gamma \text{ cm}^{-3}$)	$\text{Na}_{\text{sol}}:\text{Na}_{\text{tot}}$ (mol/mol)	$\text{Na}_{\text{sol}}:\text{Si}_{\text{sol}}$ (mol/mol)
S-3-110(16)	68	49	39%	1.69
S-3-300(16)	100	82	53%	1.49
S-3-600(16)	90	30	50%	3.65
S-3-700(16)	147	0	83%	∞

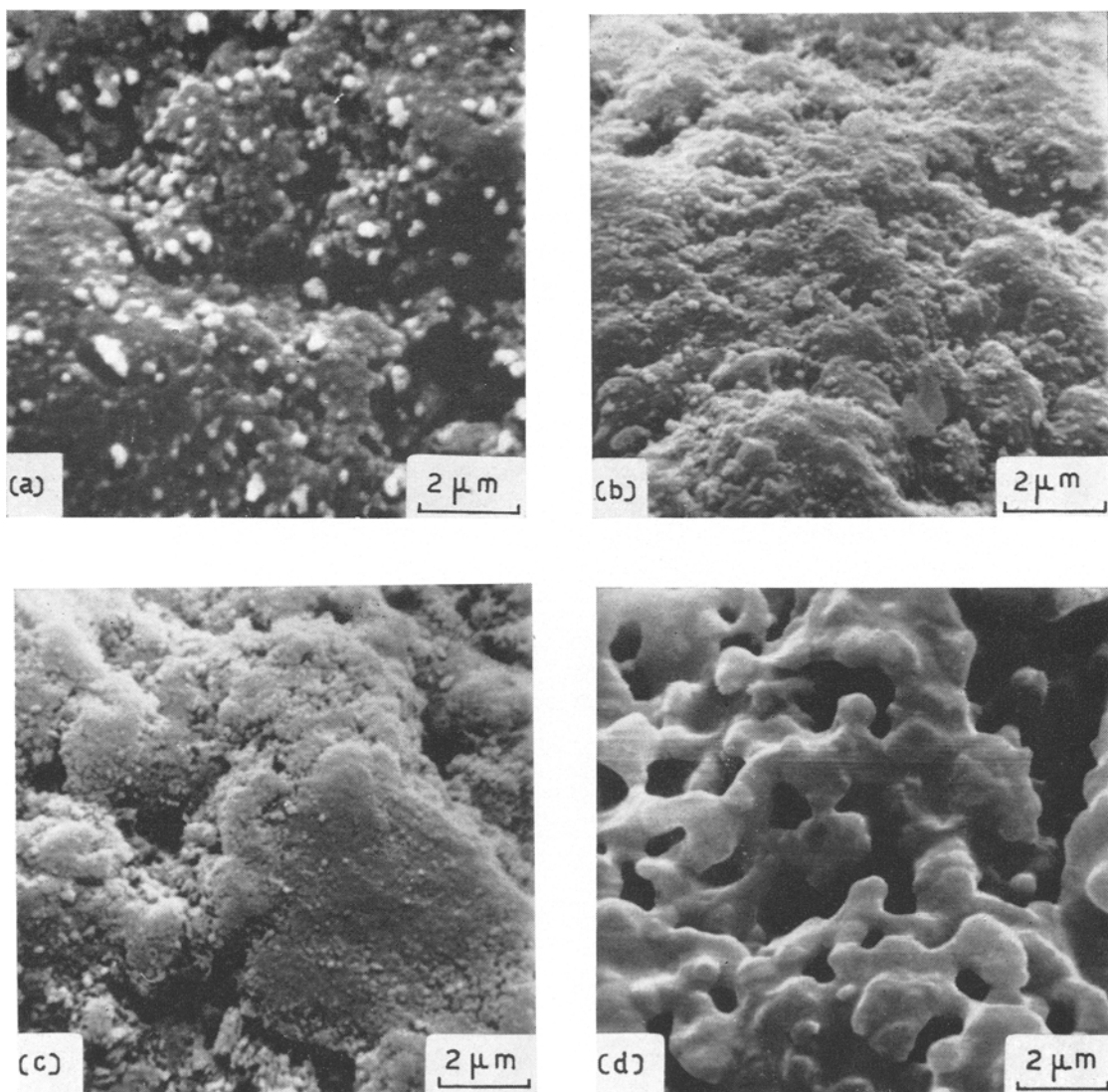


Figure 4 Scanning electron microscope observations of samples: (a) S-0-300(16); (b) S-0-1100(16); (c) S-3-600(16) (d) S-3-700(16).

contrast, Na-loaded silicas are characterized by the occurrence of considerable modifications, at much lower temperatures. X-ray diffraction spectra of Na-loaded samples reveal in fact the presence of cristobalite and quartz together with a new phase that, on the basis of known information, [32, 34] appears to be keatite. While the occurrence of the two former phases, under the given experimental conditions, has been already indicated, the presence of keatite is singular in so far as high pressures and or high concentration of bases have been claimed necessary for its

synthesis [22, 32, 33]; keatite, first discovered by Keat while investigating the recrystallization of silica under hydrothermal conditions [32, 34], has a structure containing four-fold spirals of SiO_4 tetrahedra which share corners. The essential results of the experiments are shown in Figs. 6a to e and Figs. 7a to d, constructed on a semiquantitative basis from the heights of some characteristic peaks: the relative distributions of various phases are given against main parameters time and temperature pre-treatment and NaOH content. Of special interest is Fig. 7b, which

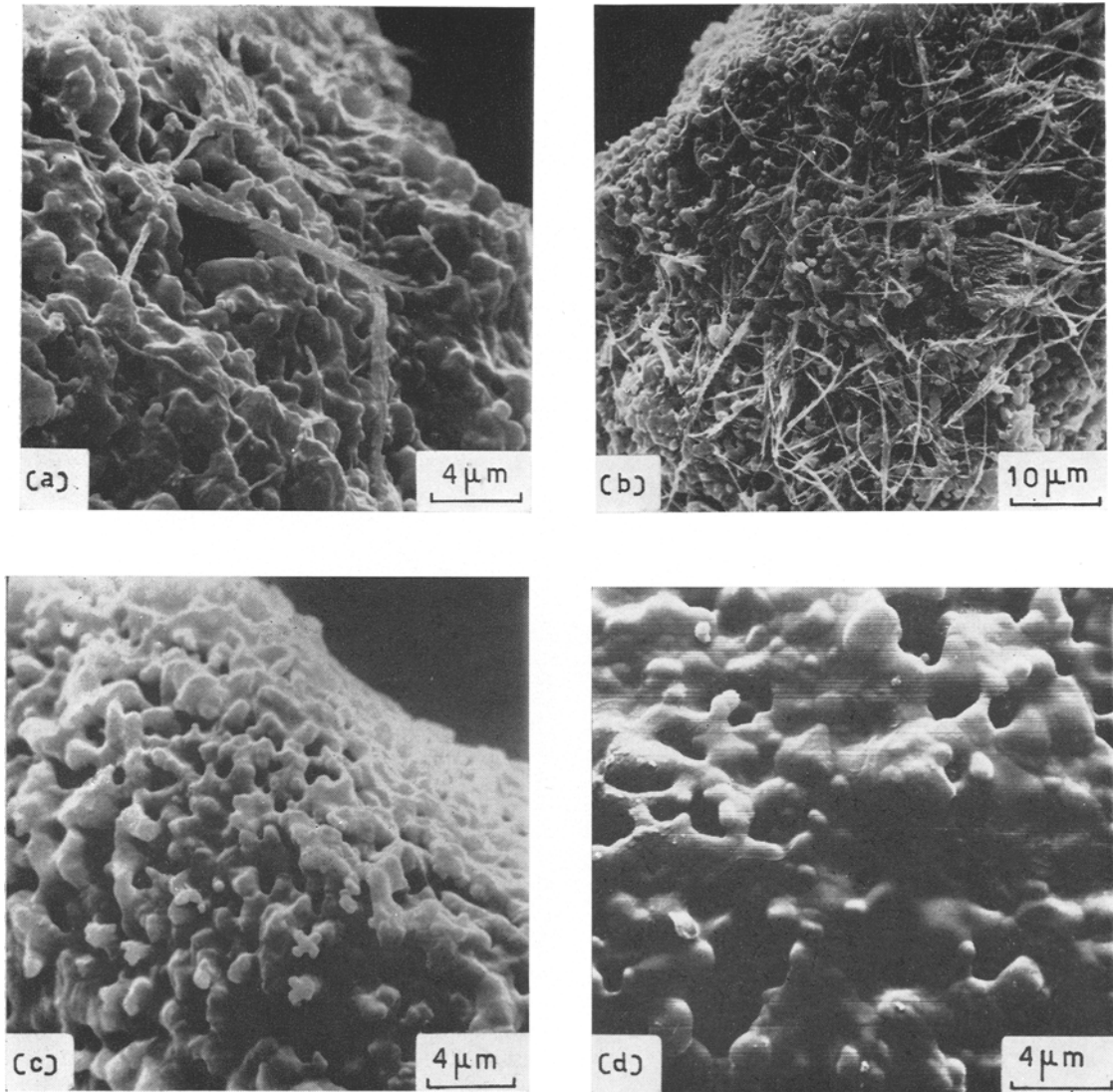


Figure 5 Scanning electron microscope observations of samples: (a) S-3-700(16); (b) S-3-700(16); (c) S-3-700(16) leached with water; (d) S-3-780(16).

shows that, as a function of pre-treatment time, the amorphous phase and cristobalite disappear, while keatite tends to decrease and quartz to increase. From it one should assume that the reaction path goes as following:

amorphous \rightarrow cristobalite \rightarrow keatite \rightarrow quartz

like that suggested by Carr and Fyfe for the case of silica treated hydrothermally under high pressure [33].

The results underline also that the forming phases depend upon mineralizer concentration:

thus keatite appears on S-1 samples, while at higher NaOH concentrations only cristobalite and quartz are present (Figs. 6c, d and e). In this range of compositions the quartz appears only after cristobalite is formed (Fig. 7c). Hence, the sequence should clearly be of the type:

amorphous \rightarrow cristobalite \rightarrow quartz

which conforms to the previous literature [18, 22]. Generally speaking, the degree of crystallization increases with time and temperature of pre-treatment as well as with NaOH concentra-

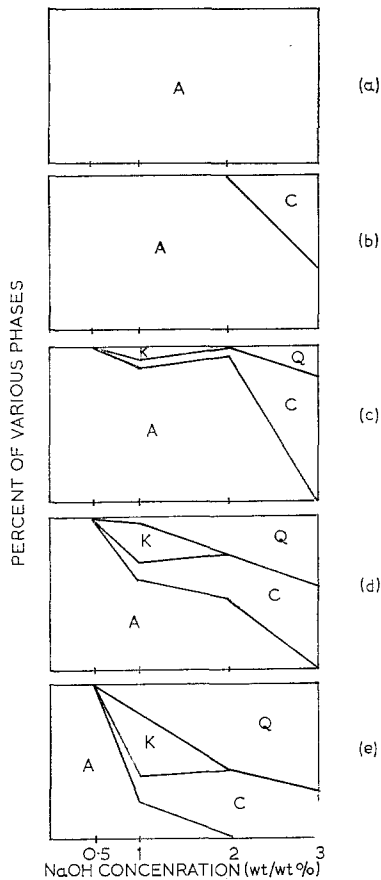


Figure 6 Crystalline phases distributions as a function of NaOH concentration of samples heat-treated: (a) at 600°C for 16 h; (b) at 650°C for 16 h; (c) at 700°C for 16 h; (d) at 700°C for 72 h; (e) at 700°C for 115 h. A: amorphous; C: cristobalite; K: keatite; Q: quartz

tion: this behaviour is clearly indicated by the fate of the amorphous phase which was found to disappear completely after 160 h (700°C) on the S-1 sample, after 115 h (700°C) on the S-2 sample and after 16 h (700°C) on the S-3 sample (Figs. 7a to d).

3.6. Optical microscopy observations

Details of the surface were investigated by optical microscopy. Making use of the information on the S-1-700, S-1-780 and S-3-700 samples activated for different lengths of time the combined results can be summarized as follows: short activation periods, as in the S-1-700(16) sample, already cause the onset of nuclei which develop into spherulites of a crystalline phase having a refractive index (n_0) between 1.48 and 1.53 (n_0 for keatite is 1.522 to 1.5113). Spherulites

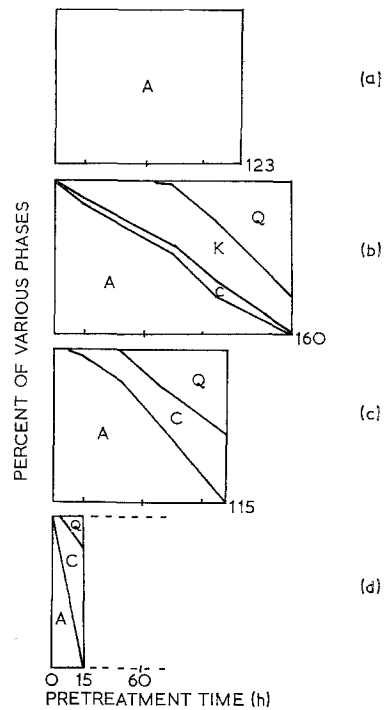


Figure 7 Crystalline phases distributions as a function of pre-treatment time of samples: (a) S-0.5-700; (b) S-1-700; (c) S-2-700; (d) S-3-700. A: amorphous; C: cristobalite; K: keatite; Q: quartz.

develop radially extending linearly through elemental particles and pores. Longer activation periods make the keatite prevail over the amorphous as shown by the S-1-700(79) sample. Onset of the quartz phase occurs on the S-1-700 (107) sample, apparently at the expense of keatite; the quartz becomes further predominant on the S-1-700(233) sample. Similar conclusions can be drawn for the S-1-780 samples. On the S-3-700(16) sample, direct observation was difficult because of the surface being completely masked by "whiskers": however, leaching with water, which dissolves them, allowed the presence of the cristobalite and quartz to be detected, which, therefore, appear to be formed at an early stage of the activation process, without the keatite being the intermediate phase.

4. Discussion

Collection of the results discussed in the text strongly indicates that loading with NaOH causes modifications in the structure of silica whilst the pure support is very stable under comparable conditions. Modifications brought

about by the "mineralizer" develop in different ways, depending upon the range of activation temperature; at lower temperatures, surface modifications appear to predominate while, at the highest temperatures, the entire mass becomes affected through processes which involve deep structural modifications.

Consider first the region of the lower temperatures ($< 600^{\circ}\text{C}$): the starting configuration (S-3-110(16)) offers evidence of a true chemical interaction between NaOH and the support: actually solubility experiments show that only a fraction of added NaOH is recovered by water leaching and that together with it some silica is dissolved. Both observations agree in indicating that, even at temperatures as low as 110°C , Na ions interact with the surface OH [5, 7, 9, 10] giving rise to silicate-type compounds: from Table I, the ratio Na/Si in solution is about 1.7. Results related to morphological properties offer additional evidence of a true chemical interaction, whose effects are already pronounced at the lower temperature of investigation (300°C). Surface areas suffer the largest variations showing losses which are almost linearly proportional to the NaOH content; since correspondingly pore volumes undergo much less pronounced variations, it is reasonable to think that the chemical interaction brings up agglomeration of the primary particles of silica, particularly of the smallest ones, so that larger particles and cavities are formed. Furthermore, a comparison of the 300°C pore size distribution curves (Figs. 2b and c) indicates that the net effect of increasing NaOH content is an enlargement of the pores.

As to the effects of temperature (over 300°C), these are better described by comparison of surface areas and pore volumes (Fig. 1): first, in the temperature range between 300 and 600°C (low temperature region) the pore volume and surface area values vary slightly thus suggesting surface modifications only, which do not alter the structure originated after the former chemical interaction with NaOH. On the contrary, the highest temperature region, whose onset can be localized somewhere between 600 and 700°C , is characterized by a sharp loss of surface area which becomes almost nil at 700°C (Fig. 1a); correspondingly, pore volume undergoes a less drastic decrease (Fig. 1b). The surface area and pore volume decrease is such that there is a considerable rise in the average radius of the pores which becomes progressively larger as the

temperature of activation increases; moreover, the distribution of pore radii broadens as indicated by the plots of Figs. 2a, b and c.

Speculation concerning the mechanism underlying these effects requires quantitative estimate of the relative variation of pore volume (dV_p) and of surface area (dS) [35]. The dV_p/dS ratio calculated from our results appears almost constant up to 600°C ; after this temperature it quickly increases, suggesting the onset of a different mechanism that can be identified as volume migration. For such an event, one should expect coalescence of elementary particles to form larger ones, Results of other techniques add further support to this interpretation: thus examination of electron micrographs of various specimens shows the agglomeration of ultimate particles into more ordered and compact structures; this results in the disappearance of surface rugosity and in the formation of larger interparticle cavities which now are entirely within the range of scanning electron microscope resolution. To this purpose, it is very interesting to compare the S-0-1100(16) and S-3-700(16) samples which are characterized by similar surface areas ($< 1\text{m}^2\text{ g}^{-1}$), but different pore volumes ($0.09\text{ cm}^3\text{ g}^{-1}$ against $0.23\text{ cm}^3\text{ g}^{-1}$).

Comparison of Figs. 4b and d clearly indicates that NaOH favours the agglomeration which, therefore, occurs at a temperature lower than in case of pure silica: possibly, this effect occurs via formation of sodium silicate fillets capable of crossing over or diffusing through interparticle spaces, when these are still large, i.e., when pore volumes are still high. On the contrary, the transport of solid material on pure silica requires close packing of the ultimate particles, i.e., pore volume almost nil. In other words, the "mineralizer" seems to act as a true interparticle ligand: this role is consistent with the chemical interaction concepts discussed above, considering that Na silicates have lower melting points and, as a consequence, lower viscosities than silica (for $\text{Na}_2\text{O-SiO}_2$ m.p. = 784°C). As a result, a volume migration occurs: this is also shown by sieving measurements (Fig. 3) that seem to confirm, in a macroscopic scale, the validity of processes assumed for the microscopic scale: thus, while on pure silica an increase of activation temperature causes shrinking of the granules and a finer particle size distribution, on Na-loaded silica, on the contrary, particles fusion results in an increase of granules size. The morphological modifications, described above in the case of

Na-loaded silicas, are accompanied by considerable structural transformations which bring about crystallization, while pure silica still remains amorphous at least up to 1100°C. Again, the "mineralizer" presence seems to play an outstanding role upon the solid phase processes. Solubility analyses which show the complete recovery of added NaOH and the absence of SiO₂ in the leaching water (S-3-700(16) sample; Table I) indicate complete decomposition of silicates; apparently, NaOH separates from the bulk, giving rise to "whiskers" which are clearly visible in the electron micrographs (Figs. 5a and b) and whose composition is confirmed by the readiness with which they dissolve in water. At this point, it seems a straightforward derivation to relate the decomposition reaction with onset of the crystallization phenomena. In this respect, useful indications come out from the already mentioned optical microscope observations which show that the crystallization evolves along radii extending linearly through silica particles and pores. Considering the coincidence with other events (absence of silica in the leaching water, formation of "whiskers", etc.), it seems reasonable to identify the nuclei of the crystallization with those same sites where decomposition of silicates starts occurring. While, on a qualitative basis, the crystallization process can be solely described by the onset of said nuclei, the examination of X-ray results shows that the nature of the forming phases and the degree of crystallization are dictated by an interplay of other parameters such as cation concentration, temperature and time of pre-treatment. Once a crystalline phase is formed, it evolves along a path dictated by the sequence of the free energies at the given temperature, according to Ostwald's rule, as emphasized by DeKeyser and Cypres [18]. The foregoing results and literature information [18, 22] indicate that the phase sequence obeyed by the S-2 and S-3 samples should be of the type:

amorphous → cristobalite → quartz.

A notable exception is offered by the S-1 samples wherein the presence of keatite has been clearly demonstrated; its presence is contrary to expectation as in previous works keatite has been formed only in case of silicas activated under more drastic conditions, i.e., high pressures and high "mineralizer" content [22, 32, 33]. The presence of keatite in our samples suggests that under the indicated conditions, the most prob-

able sequence is:

amorphous → cristobalite → keatite → quartz.

It cannot be excluded, however, that keatite also forms directly from the amorphous phase.

Undoubtedly, the observed behaviour requires further elucidation of the mechanism and transitions in the crystallization of silicas; current efforts on the subject of "mineralizer"-silica systems and their catalytic significance will be directed, amongst others, to demonstrate if keatite is a more or less common step in the sequence.

Acknowledgements

The authors gratefully acknowledge J. Bart, R. Covini, A. Marzi, and O. Pilati for their helpful comments and O. Della Noce, G. Ficcagna, G. Sgrinzato, M. Solari, A. Targa, and D. Volo for the measurements by various techniques.

References

1. G. MOUGEY, J. FRANÇOIS-ROSSETTI, and B. IMELIK, "The Structure and Properties of porous Materials", Colston Paper 1958 (Butterworths, London, 1958) p. 266.
2. J. GODON-RENOU, J. FRAISSARD, J. FRANÇOIS-ROSSETTI, and B. IMELIK, *Bull. Soc. Chim.* **1962** (1962) 1156.
3. J. UYTTERHOEVEN and J. ANDRE, *Bull. Groupe Fran. Argiles* **15** (1964) 11. *Chem. Abs.* **62** 15466f.
4. M. MUROYA and S. KONDO, *Bull. Chem. Soc. Japan* **43** (1970) 3453.
5. S. A. GREENBERG, *J. Phys. Chem.* **60** (1956) 325.
6. N. HENRY and R. A. ROSS, *J. Chem. Soc.* **1962** (1962) 4265.
7. D. L. DUGGER, J. H. STANTON, B. N. IRBY, B. L. MCCONNELL, W. W. CUMMINGS, and R. W. MAATMAN, *J. Phys. Chem.* **68** (1964) 757.
8. V. A. FLORINSKAYA, *Stek. Sos. Akad. Nauk. SSSR* **1964** (1965) 13. *Chem. Abs.* **64**, 4750e.
9. H. TITTIEN, *J. Phys. Chem.* **69** (1965) 350.
10. R. W. MAATMAN, *ibid* **69** (1965) 3196.
11. G. M. MATVEEV and A. S. AGARKOV, *Izv. Akad. Nauk. SSSR. Neorg. Mater.* **4** (1968) 406. *Chem. Abs.* **69** 22620d.
12. T. YANAGASE, Y. SUGINOHARA, and K. NAKAMURA, *Nippon Kinzoku Gakkaishi* **32** (1968) 379. *Chem. Abs.* **69**, 37989c.
13. R. HAYAMI, T. OGURA, and R. TERAJ, *Zairyo* **17** (1968) 521.
14. R. TERAJ, I. SUGAE, and R. HAYAMI, *ibid* **17** (1968) 527.
15. I. P. ALEKSEEVA and A. P. DUSHINA, *Kolloid. Zh.* **31** (1969) 483.
16. M. J. WYART, *Bull. Soc. France Min.* **67** (1944) 367.
17. A. DIETZEL and H. WICKERT, *Glastech. Ber.* **29** (1956) 1.

18. W. L. DEKEYSER and R. CYPRES, *Silic. Indus.* **5** (1961) 237.
19. O. W. FLOERKE, *Ber. Deutsch. Keram. Ges.* **38** (1961) 89.
20. Y. SUSUKI and K. MURANAKA, *Asahi Garasu Kenkyu Hokoku* **14** (1964) 59. *Chem. Abs.* **62**, 14259g.
21. R. WOLLAST, *Epitoanyag* **18** (1966) 53. *Chem. Abs.* **65**, 16635d.
22. B. SIFFERT and R. WEY, *Silic. Indus.* **32** (1967) 415.
23. Y. NURISHI, T. NISHIZAWA, H. SEKIYA, and T. HIBINO, *Kogio Kagaku Zasshi* **71** (1968) 662. *Chem. Abs.* **69**, 45773v.
24. Y. NURISHI, E. MIURA, K. AZUMA, and T. HIBINO, *Kogio Kagaku Zasshi* **71** (1968) 666. *Chem. Abs.* **69**, 45742j.
25. S. KUMAR and B. B. NAG, *Trans. Ind. Ceram. Soc.* **27** (1968) 103. *Chem. Abs.* **70**, 108748j.
26. T. NEGAS and C. A. SORREL, *J. Amer. Ceram. Soc.* **51** (1968) 622.
27. T. SUGIMURA and I. MAKI, *Asahi Garasu Kogyo Gijutsu Shorei Kai Kenkyu Hokoku* **14** (1968) 89. *Chem. Abs.* **71** 104669g.
28. J. F. CORWIN, R. G. YALMAN, J. W. EDWARDS, and G. E. OWEN, *J. Phys. Chem.* **61** (1957) 939.
29. R. G. YALMAN and J. F. CORWIN, *ibid* **61** (1957) 1432.
30. F. M. NELSEN and F. T. EGGERTSEN, *Analyt. Chem.* **30** (1958) 1387.
31. American Petroleum Institute, "Physical Properties of Cracking Catalysts: A Progress Report" (1959) p. 37.
32. P. P. KEAT, *Science* **120** (1954) 328.
33. R. M. CARR and W. S. FYFE, *Amer. Mineral* **43** (1958) 908.
34. J. SHROPSHIRE, P. P. KEAT, and P. A. VAUGHAN, *Z. Krist.* **112** (1959) 409.
35. W. G. SCHLAFFER, C. Z. MORGAN, and J. N. WILSON, *J. Phys. Chem.* **61** (1957) 714.

Received 6 November and accepted 25 January 1973.